This article has been accepted for inclusion in a future issue of this journal. Content is final as presented, with the exception of pagination.

Hybridization of Multiconductor Transmission Line Solver With Circuit Solver Ngspice to Treat Line Interconnections and Terminations

Alberto Gascón Bravo, Luis Manuel Diaz Angulo, *Member, IEEE*, Ferran Silva, *Senior Member, IEEE*, Marcos Quílez, *Member, IEEE*, Kenan Tekbaş, *Member, IEEE*, and Salvador G. García, *Senior Member, IEEE*

***Abstract*—This article presents the hybridization of a multiconductor transmission line (MTL) solver, implemented using the finite-difference time-domain method, with the circuit solver ngspice to treat the terminations and interconnections of transmission lines. Transient analysis and crosstalk in MTLs have been widely studied, but the line terminations and the connections between lines are mostly restricted to lumped resistors, inductors and capacitors (RLC) components. However, realistic systems, such as power distribution or communication systems, typically involve more complex and a priori unknown connections. By integrating the MTL solver with a circuit solver, the proposed approach enables the inclusion of any component for which a circuit model can be written or already exists, i.e., dispersive elements, such as ferrites, and electronic components, such as diodes, amplifiers, or transistors. This capability makes it possible to simulate the MTL networks with complex, including nonlinear, terminations and interconnections modeled by circuits. The proposed method is validated through comparison with experimental laboratory measurements.**

***Index Terms*—Circuit simulators, computational modeling, finite difference methods, multiconductor transmission lines (MTLs), time-domain analysis.**

I. Introduction

Modern industries, from automotive and aerospace to communication and power distribution, use sophisticated cable systems composed of networks of cable bundles interconnected by electrical and electronic circuits. These systems play a crucial role in electromagnetic compatibility (EMC) assessments, both as victims of interferences that might affect connected equipment and as potential emitters of interferences. The increasing speed, bandwidth and complexity of the electronic components used in cable systems, along with higher operating frequencies, make them even more critical components that cannot be neglected in full-wave simulations of large-scale systems.

The finite fifference time fomain (FDTD) method [1], [2] is one of the most powerful and widely used numerical methods to simulate 3-D electromagnetic problems. Cable networks can be represented as a series of multiconductor transmission lines (MTL), the currents and voltages in the MTL being described using transmission line theory, which can be solved using FDTD method as well. There are many successful examples of the hybridization of full-wave FDTD solvers with MTL solvers [3], [4], [5], [6], [7]. However, the modeling of terminations and interconnections of the TLs are not adequate to describe the behavior of the electronic systems in realistic cable networks. The general solution, and the particular solution for resistive loads, has been studied in detail [8]. For transmission lines connected by loads consisting of combinations of resistors, inductors and capacitors, solutions make use of the state-variable formulation [9], [10], [11] or the modified nodal analysis [12]. The inclusion of dispersive elements can be done using the Prony method [13], [14] or recurring to the piecewise-linear recursive convolution method [15]. This limitation of state-of-the-art MTL solvers hinders the simulation of realistic transmission line networks with arbitrary terminations and interconnections.

There are two main strategies to simulate transmission lines connected by circuits with electronic components. One is including TL equations into circuit solvers [16]. This approach suffers from a simplistic TL description, constrained to the capabilities of the circuit solver and is not suitable to be hybridized with a 3-D full-wave solver. The other strategy entails coupling the TL solver with an external circuit solver. The issue with the latter is that electromagnetic solvers with this capability use dedicated circuit solvers that do not offer the possibility of including arbitrary components and are proprietary software that cannot be modified to include more components [6], [17], [18], [19].

Received 29 November 2024; revised 27 February 2025 and 2 April 2025; accepted 2 April 2025. This work was supported by PID2022-137495OB-C31 funded by MICIU/AEI/10.13039/501100011033 and by ERDF, EU, in part by the EU Horizon 2020 Research and Innovation Program through Marie Sklodowska Curie Action under Grant 101066571, in part by the European Union under Grant 101101961 - HECATE, in part by the Clean Aviation Joint Undertaking and its Members, and in part by Universidad de Granada / CBUA. *(Corresponding author: Alberto Gascón Bravo.)*

Alberto Gascón Bravo, Luis Manuel Diaz Angulo, and Salvador G. García are with the Group of Electromagnetism of Granada (GEG), University of Granada, 18012 Granada, Spain (e-mail: agascon@ugr.es; lmdiazangulo@ugr.es; salva@ugr.es).

Ferran Silva and Marcos Quílez are with the Electromagnetic Compatibility Group (GCEM), Universitat Politècnica de Catalunya (UPC), 08034 Barcelona, Spain (e-mail: ferran.silva@upc.edu; marcos.quilez@upc.edu).

Kenan Tekbaş is with the Group of Electromagnetism of Granada (GEG), University of Granada, 18012 Granada, Spain, and also with the Department of Electrical and Electronic Engineering, Amasya University, 05100 Amasya, Türkiye (e-mail: kenan.tekbas@ugr.es).

Color versions of one or more figures in this article are available at https://doi.org/10.1109/TEMC.2025.3560361.

Digital Object Identifier 10.1109/TEMC.2025.3560361

To tackle these shortcomings, in this article we propose the hybridization of an FDTD MTL solver (MTL-FDTD, from now on) with a SPICE-based open-source simulator for electric and electronic circuits, ngspice [20]. SPICE is the origin of most modern electronic circuit simulators, its successors being widely used in the electronics community. In ngspice, models of electronic components (netlists), easily accessible and provided by both the manufacturers and the open-source community, can be used to simulate discrete circuits [21]. Thus, most existing electronic components but also new components can be simulated. Coupling the MTL-FDTD solver with ngspice offers the possibility of including nonlinear and active components in the connections between the MTLs, and of simulating the effect of external perturbations, such as plane waves, which MTL-FDTD naturally incorporates as distributed voltage sources, on the electronic components. The core idea of the hybridization is the following: at each time step, the MTL-FDTD solver computes the current at all points of the transmission lines, and the voltages at all points except the extremes. The circuit solver is passed the currents at the extremes of the transmission lines, and produces the voltages at said points. It should be stressed that albeit the MTL-ngspice solver can be used on its own, this solver is integrated into an open-source 3-D full-wave FDTD solver [22] (3-D-FDTD, from now on), allowing to simulate the interaction of MTL networks with transient electromagnetic fields in a 3-D domain. However, the description of the whole hybridization, 3-D-FDTD/MTL-FDTD/ngspice, lies beyond the scope of this article, where we focus on the implementation details of the interface between the MTL solver and the circuit solver.

The rest of this article is organized as follows. Section II describes the MTL-FDTD model and the hybridization with ngspice. Section III presents the validation of the hybridized approach comparing simulations against measured data in three different cases: a single conductor transmission line terminated with a diode, a single conductor transmission line terminated with an operational amplifier, and a two conductor line, where one line is excited, and the other line is terminated with an operational amplifier. Finally, Section IV concludes this article.

II. MTL Model and Interfacing Procedure

The MTL theory relates the voltages and currents on each conductor of a MTL under the assumption that the conductors have a constant cross-section and that the propagation mode is quasi-TEM. For a multiconductor line with $N+1$ lossy conductors (N conductors plus a reference conductor), those relations can be written in the following form:

$$\frac{\partial\{\mathrm{V}\}}{\partial z} + [\mathrm{R}]\{\mathrm{I}\} + [\mathrm{L}]\frac{\partial\{\mathrm{I}\}}{\partial t} = 0 \tag{1a}$$

$$\frac{\partial\{\mathrm{I}\}}{\partial z} + [\mathrm{G}]\{\mathrm{V}\} + [\mathrm{C}]\frac{\partial\{\mathrm{V}\}}{\partial t} = 0 \tag{1b}$$

where [L] and [C] are the per-unit-length inductance and capacitance between all conductors and [R] and [G] are the per-unit-length losses: resistance (along conductors) and conductance (between conductors). $\{\mathrm{V}\}(z,t) = [V_1 V_2 \ldots V_N]^T$ is the vector of the voltages of each conductor with respect to the reference conductor, and $\{\mathrm{I}\}(z,t) = [I_1 I_2 \ldots I_N]^T$ is the vector of the currents on those conductors. [L], [C], [R], and [G] can vary along the line length without varying the cross-section, describing a nonhomogeneous transmission line. To a greater or lesser extent all the per-unit-length parameters are frequency dependent: [R] and [L] through the skin effect, [C] and [G] due to dielectric losses [23]. Since it will not affect the discussion of the interfacing with ngspice, for the sake of simplicity we will assume that the lines are uniform and homogeneous, and that their properties are frequency independent.

The equations in (1) are discretized using the finite-difference time-domain technique applied to transmission lines (MTL-FDTD) described in [24]. The solution time is divided into N_t segments of length Δ_t and the transmission line is divided into N_z segments of length Δ_z. There are N_z+1 voltage nodes (at the extreme of the segments) and N_z current nodes (at the center of the segments). The final discretized voltage and current equations are

$$\{\mathrm{I}\}_k^{n+3/2} = F_{I+}^{-1}[F_{I-}\cdot\{\mathrm{I}\}_k^{n+1/2} - (\{\mathrm{V}\}_{k+1}^{n+1} - \{\mathrm{V}\}_{k+1}^{n})] \tag{2a}$$

$$\text{for } k = 1, 2, \ldots, N_z \text{ and} \tag{2b}$$

$$\{\mathrm{V}\}_k^{n+1} = F_{V+}^{-1}[F_{V-}\cdot\{\mathrm{V}\}_k^{n} - (\{\mathrm{I}\}_k^{n+1/2} - \{\mathrm{I}\}_{k-1}^{n+1/2})] \tag{2c}$$

for $k = 2, 3, \ldots, N_z$. Thus, (2b) is only valid for internal voltage nodes of the line. In the equations above

$$F_{V\pm} = \left(\frac{\Delta z}{\Delta t}[\mathrm{C}] \pm \frac{\Delta z}{2}[\mathrm{G}]\right) \tag{3a}$$

$$F_{I\pm} = \left(\frac{\Delta z}{\Delta t}[\mathrm{L}] \pm \frac{\Delta z}{2}[\mathrm{R}]\right). \tag{3b}$$

Equations (2) are solved in a leapfrog fashion, i.e., first the voltages along the line are obtained (2b) at time step $n+1$ in terms of the previous time steps (V^n, $I^{n+1/2}$). Then, the currents are obtained (2a) in terms of the voltages obtained from (2b) (V^{n+1}) as well as previously obtained values (V^n, $I^{n+1/2}$). The solution starts with an initially relaxed line having zero voltage and current values.

A. *Ngspice Interface for Terminations and Interconnections*

The equations above describe a single MTL, not taking into account its terminations or the connections to other transmission lines. Hence, the terminal conditions have to be incorporated. We will use the term *junction* to refer indistinctly to terminations and interconnections since their treatment is the same. As can be seen in Fig. 1, the essential problem in incorporating the terminal conditions is that in the MTL-FDTD discretization the voltage and current of the first ($\{V_1, I_1\}$) and last ($\{V_{N_Z+1}, I_{N_Z}\}$) node of the transmission line are not collocated neither in space or time. However, the terminal conditions relate the voltage of the first node to the current of the source (V_1, I_S) and the voltage of the last node to the current of the load (V_{N_Z+1}, I_L), and these pairs of voltage and current are collocated in time and space.

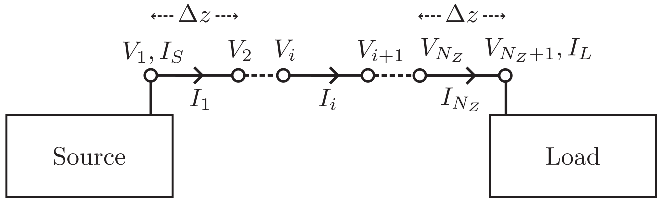

Fig. 1. Discretized transmission line showing source and load currents, collocated in time and space with the voltages at the extremes of the line.

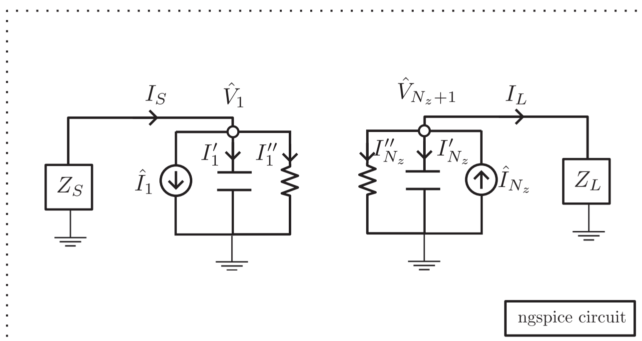

Fig. 2. Equivalent circuit of the extreme of a transmission line.

If we apply the spatial discretization to (1b) at the extremes of the line (source and load, respectively), we obtain

$$\frac{I_1^{n+1/2} - I_S^{n+1/2}}{\Delta z/2} + C\frac{\partial V_1^{n+1/2}}{\partial t} + GV_1^{n+1/2} = 0 \tag{4a}$$

$$\frac{I_L^{n+1/2} - I_{N_z}^{n+1/2}}{\Delta z/2} + C\frac{\partial V_{N_z+1}^{n+1/2}}{\partial t} + GV_{N_z+1}^{n+1/2} = 0. \tag{4b}$$

In the discretization of the spatial derivative, the denominator is $\Delta z/2$ because the source (load) current is on the first (last) voltage node, and hence, separated only $\Delta z/2$ from the adjacent current segment. From this discretization, the update relations for the current at the source and the load can be derived

$$I_S^{n+1/2} = I_1^{n+1/2} + C\frac{\Delta z}{2}\frac{\partial V_1^{n+1/2}}{\partial t} + G\frac{\Delta z}{2}V_1^{n+1/2} \tag{5a}$$

$$I_L^{n+1/2} = I_{N_z}^{n+1/2} - C\frac{\Delta z}{2}\frac{\partial V_{N_z+1}^{n+1/2}}{\partial t} - G\frac{\Delta z}{2}V_{N_z+1}^{n+1/2}. \tag{5b}$$

Since, we want to hybridize with a circuit solver, we will describe (5a) and (5b) in terms of their circuit equivalent. Each of (5a) and (5b) represents a node equation with four currents: the current at the source (load), the current of the first (last) segment of the transmission line, the current through a capacitor with value $C' = C\Delta z/2$ and the current through a resistor with value $R' = (G\Delta z/2)^{-1}$ [25]. Fig. 2 shows the circuit equivalent of the extremes of the transmission line, where Z_S and Z_L represent the impedance of the terminations connected at source and load ends of the line, respectively. To avoid confusions between the voltages and currents shared between the MTL and the ngspice domains, we will refer to the latter as $\hat{V}$ and $\hat{I}$. The currents in the circuit are defined as

$$\hat{I}_1' = \frac{1}{2}C\Delta z\frac{\partial \hat{V}_1}{\partial t} \tag{6a}$$

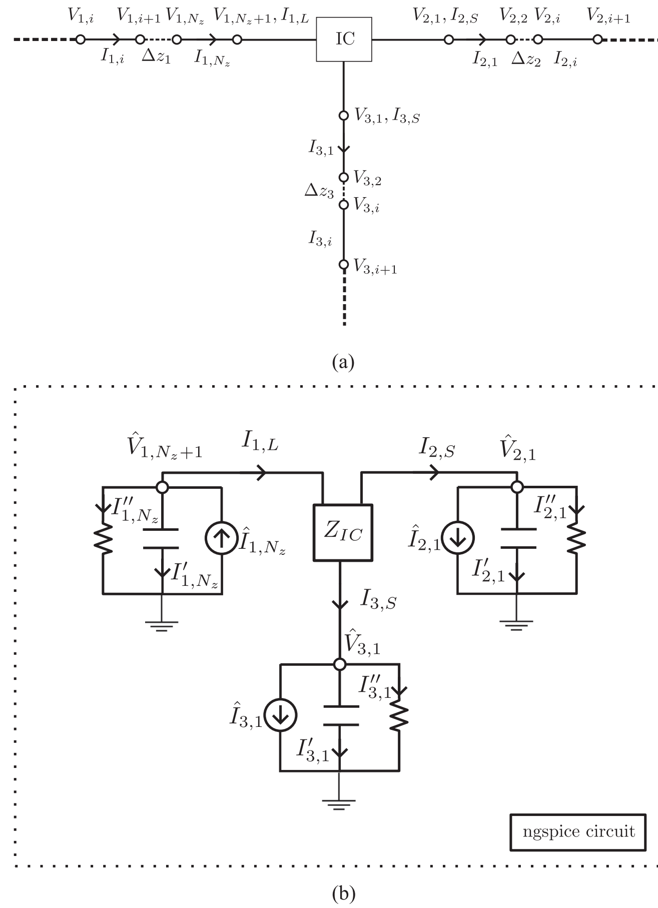

Fig. 3. Extrapolation of the discretization procedure to more than one transmission line. (a) Discretization of the extremes of three interconnected transmission lines. (b) Equivalent circuit of the interconnection of three transmission lines.

$$\hat{I}_1'' = \frac{1}{2}G\Delta z\hat{V}_1 \tag{6b}$$

$$\hat{I}_{N_z}' = \frac{1}{2}C\Delta z\frac{\partial \hat{V}_{N_z+1}}{\partial t} \tag{6c}$$

$$\hat{I}_{N_z}'' = \frac{1}{2}G\Delta z\hat{V}_{N_z+1}. \tag{6d}$$

Now, that we have a circuit description of the TL, we can use the circuit solver to update the voltages on the circuit nodes ($\hat{V}_1$ and $\hat{V}_{N_z+1}$) that correspond to the voltages of the extremes of the line (V_1 and V_{N_z+1}). The circuit represented in Fig. 2 is defined in ngspice, with Z_S and Z_L any user-defined circuits. At each time step, the value of the current sources ($\hat{I}_1$ and $\hat{I}_{N_z}$) are modified to the value of the corresponding current segment from the MTL-FDTD simulation. Then, the circuit is evolved to next time step, producing the voltages corresponding to the line extremes, which are read and passed to the MTL-FDTD algorithm.

This procedure is easily scalable to interconnections between transmission lines. In that case, the procedure is the same but each junction circuit is connected to a circuit representing a transmission line, one for each transmission line connected to the interconnection. Fig. 3(a) shows an example of three interconnected transmission lines, analogous to Fig. 1, where IC is any interconnection between the transmission lines. For lines beginning (ending) at the IC, it will be equivalent to the source (load) in Fig. 1. In Fig. 3(b) we have represented the three circuits connected to the same Z_{IC}, where Z_{IC} represents the impedance of the interconnection between the transmission lines. This connection could represent any kind of connection between the circuits, i.e., they could be connected to the same inner point through lumped components, or they could be connected to a three-port electronic component. Dispersive elements whose properties are complicated to model using combinations of resistors, inductors and capacitors (RLC) elements (such as ferrites) can be included using a netlist description. In this way, ferrite beads and chokes around the wires can be simulated as well, using an interconnection to split the MTL at the position of the component.

B. Algorithm

Using the discretization of the MTL equations in (2) in combination with the circuit representation of the extremes of the transmission line provided by ngspice, a solution for MTLs with arbitrary interconnections and terminations can be constructed.

At each time step the current source representing the current at the extreme of the transmission line, $\hat{I}_{i,k}$, is updated. Then, the circuit advances a time step and the corresponding voltage ($\hat{V}_1$ or $\hat{V}_{N_z+1}$) is returned. The inner state of the circuit is maintained between time steps; otherwise, components, such as capacitors, inductors, and other nonlinear components, whose behavior depend on the time evolution of the circuit could no be simulated.

The iterative procedure to update currents and voltages is as follows.

1) Advance $\{V\}_k^{n+1}$ $(k = 2 \dots N_z)$ for each transmission line using the discretized expression in (2b);
2) Advance $\{V\}_1^{n+1}$ and $\{V\}_{N_z+1}^{n+1}$ for each transmission line solving all ngspice circuits follows:
   - for each TL attached to a junction, update the corresponding current source $\hat{I}_{i,k}$, using the current of the transmission line segment attached to that node, $I_{i,k}^{n+1/2}$, with $k = 1, k = N_z$, and i corresponding to the TL;
   - advance the transient ngspice simulation by Δt;
   - assign each $\hat{V}_{i,k}$ to the corresponding voltage on the transmission line $V_{i,k}^{n+1}$ $(k = 1$ or $k = N_z)$.
3) Advance $\{I\}_k^{n+3/2}$ $(k = 1 \dots N_z)$ for each transmission line using the discretized expression in (2a).

III. Validation

The proposed method is validated against simulations and measurements. The MTL solver should reproduce the results of benchmark simulations performed with other simulators, and whose results are well known. Since the goal of the MTL solver is to be eventually integrated into a 3-D-FDTD solver, we have chosen to compare it against simulations performed with [22]. We will use a setup consisting of a thin wire over a ground plane.

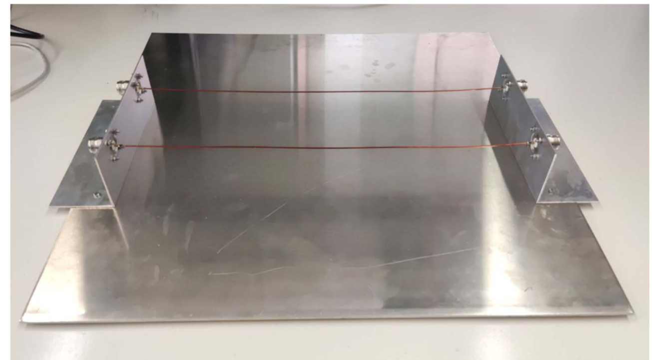

(a)

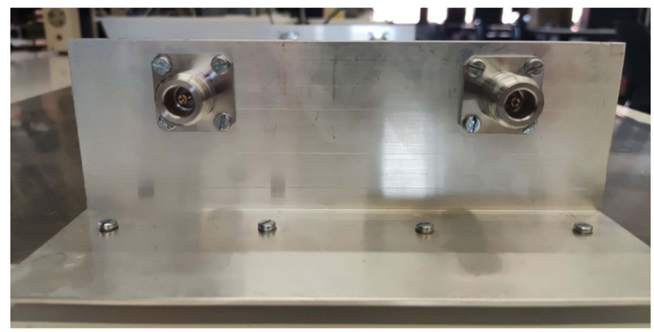

(b)

Fig. 4. Experimental setup. (a) Top view of the wire panel. (b) Side view of the wire panel.

For the experimental validation, the measurements were performed at the GCEM-UPC laboratory [26]. The validation uses three different setups: a one-conductor transmission line terminated with a diode (Section III-D1), a one-conductor transmission line terminated with a operational amplifier (op-amp, from now on, Section III-D2), and a two-conductor transmission line, where we measured the crosstalk between the excited line and the receptor line, which is terminated with an op-amp (Section III-D3).

To facilitate the reproducibility of our method, the implementation of the solution along with the measured data and the necessary framework to reproduce the validation cases can be found at [22].

A. Code Implementation

The MTL solver is written in Fortran and integrated in a broader open-source electromagnetic suite, *opensemba* [22]. This suite contains, among others, a 3-D-FDTD solver, SEMBA-FDTD [22], a state-of-the-art, general-purpose time-domain simulator developed and validated by the GEG team [27] for various applications [28], [29], [30].

B. Measurement Setup

The measurement setup consists on an aluminum sheet with two L-shaped profiles. Two wires connect the two profiles, attached to N-type ports (Fig. 4). The wires are 40 cm long, separated 10 cm and positioned 4 cm above the ground plane.

This article has been accepted for inclusion in a future issue of this journal. Content is final as presented, with the exception of pagination.

Losses in the wires are considered to be negligible, and the per-unit-length inductance and capacitance matrices, referred to the sheet below them, are as follows:

$$L = \begin{bmatrix} 938.95 & 39.87 \\ 39.87 & 938.95 \end{bmatrix} \text{nH} \tag{7a}$$

$$C = \begin{bmatrix} 11.87 & -0.504 \\ -0.504 & 11.87 \end{bmatrix} \text{pF.} \tag{7b}$$

These values have been computed using a dedicated electrostatic solver, and their values match those of the theoretical expressions for two wires over a ground plane [31]. The type *N* ports at the end of the lines can be left open, can be connected to $50\,\Omega$ loads, or can be connected to a circuit. With this setup, propagation in a single wire and cross-talk between the wires can be measured. For data acquisition a *Rhode & Schwarz RTC1002* oscilloscope was used [32]. In Sections III-D1 and III-D2 the signal generator integrated in the oscilloscope was used. In Section III-D3 a signal generator reaching higher frequencies was needed, and a *Agilent 33220 A* signal generator was used [33].

C. Validation Against Simulations

First, we have validated the MTL-FDTD solver against a 3-D-FDTD solver with a different implementation of wires. In the 3-D-FDTD solver *opensemba*, wires are modeled using Holland's thin-wire formalism [34]. The experimental setup in Fig. 4 was reproduced [see Fig. 5(a)], with the simulation domain composed of $24 \times 24 \times 24$ cubic cells, each with a size of $\Delta l = 4\,$cm, truncated by PML boundary conditions. The ground plane is a PEC surface. A wire is left open on both ends, while the other is excited with a voltage source and terminated with $50\,\Omega$ resistors at both ends. The voltage source is a sinusoidal waveform with a frequency of $100\,$kHz and an amplitude of $10\,$V. Since one wire is open at both ends, the effect of the L-shaped profiles will be that of closing the current loop on the connected wire. Thus, for the sake of simplicity, we simulated the profiles as two vertical segments at the ends of the excited wire, which should have the same effect. The simulation runs for 2×10^5 steps with a time step of $\Delta t = 10\,$ps.

In the MTL-FDTD simulation, the domain is 1-D and composed of 24 segments with $\Delta z = 4$ cm. Instead of simulating the ground plane, the MTL-FDTD solver uses the inductance and capacitance matrices of the system. The setup with only one wire connected to the ground plane can be represented as a one-conductor transmission line, whose inductance and capacitance are given in (7).

In both simulations, we probe the current at the end of the excited wire. Fig. 5(b) shows the results obtained with the 3-D-FDTD solver and the MTL-FDTD solver, which are in perfect agreement.

D. Validation Against Measurements

1) Diode: To validate this scenario, we have used the setup shown in Fig. 6(a). One wire is excited with a sinusoidal waveform with amplitude equal to 5 V and frequency 50 kHz in series with a $50\,\Omega$ resistor (inner resistance of the source). A zener diode is connected to the other end of the wire, which is grounded. To simulate the zener diode we have used the model for diodes included in ngspice with the following parameters: breakdown voltage $V_B = 3.966\,$V, saturation current $I_s = 193.4\,$fA, resistance $R = 0.1\,\Omega$, zero-bias junction bottom-wall capacitance $C_{J0} = 239.5\,$pF, breakdown emission coefficient $N = 13$ and current at breakdown voltage $I_{\text{BV}} = 64.74\,$mA. These parameters are adapted from the parameters found for zener diodes with breakdown voltage $3.9\,$V found at [35], [36].

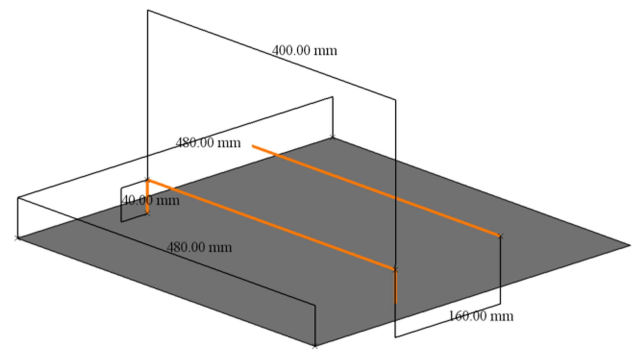

(a)

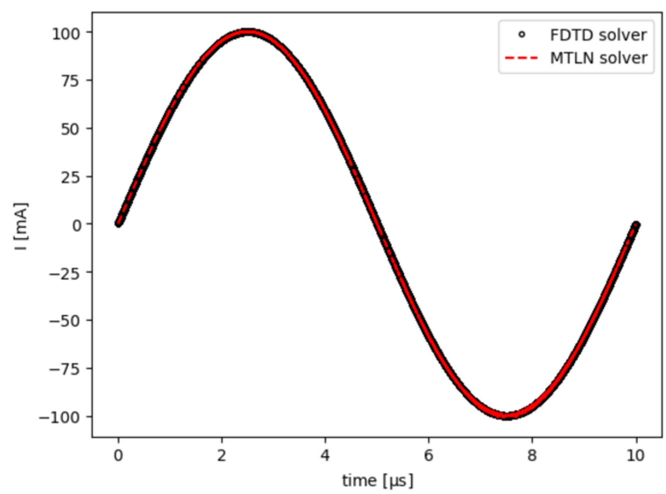

(b)

Fig. 5. FDTD simulation setup and results using the 3-D-FDTD solver and the MTL-FDTD solver. (a) Experimental setup simulated in FDTD. (b) Current at wire end.

Fig. 7 shows the voltage drop at the diode, compared with the simulated values. Both the clipping at $\simeq 0.7\,$V characteristic of silicon diodes, and the clipping at the reverse breakdown voltage can be observed.

2) Operational Amplifier: The use of op-amps is widespread. In this work, we use them as a benchmark for the inclusion of electronic components in the terminations of transmission lines. Op-amps can be saturated, which introduces nonlinearities in the problem. This is particularly interesting since it represents a phenomenon customarily found in electronic circuits, which is absent in TL solvers. To validate the simulation of op-amps, we have used a commercially available operational amplifier from *Texas Instruments*, model *TL071cp* [37], in a setup as that shown in Fig. 6(b). The wire is excited on one end with a sinusoidal

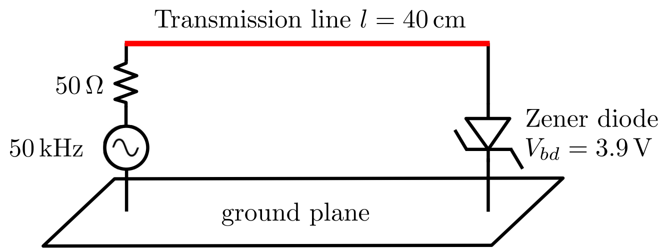

(a)

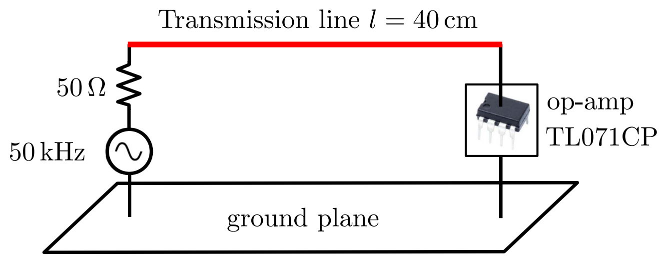

(b)

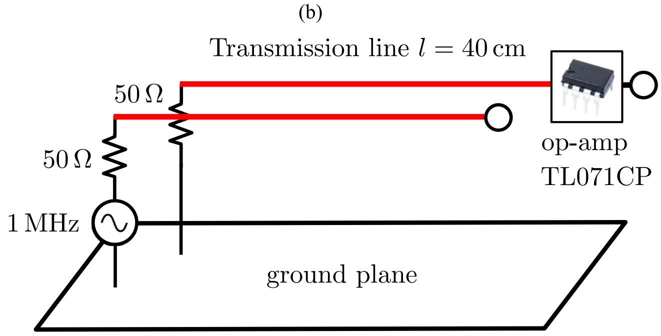

(c)

Fig. 6. Schematic of measured circuits. (a) Single wire terminated with a diode. (b) Single wire terminated with a op-amp. (c) Two-conductor line. One wire is connected to the source and acts as the interference generator. The receptor wire is terminated with an op-amp.

waveform with frequency $50\,\mathrm{kHz}$ and two different amplitudes. The op-amp is at the other end, where we measure its input and output. The op-amp is powered with $\pm\,15\,\mathrm{V}$ and configured to work as a inverting amplifier with an amplification factor of 10. To simulate the op-amp we have used the model provided by the manufacturer [38]. This model emulates the performance of the device included its nonideal behavior, such as output saturation and frequency-dependent gain.

Fig. 8 shows the simulated and measured input and output voltages of the op-amp, for two different input voltages. When the amplitude of the input voltage is $0.2\,\mathrm{V}$, the op-amp works in the linear regime. However, when the amplitude of the input voltage is $2\,\mathrm{V}$, the amplified voltage would be $20\,\mathrm{V}$, so the op-amp should saturate at $15\,\mathrm{V}$.

3) Cross-Talk: Transmission line solvers typically include the capability to compute the cross-talk between conductors of a transmission line. However, the capability to compute the interferences caused in an electronic component due to the signal carried by a nearby wire is a novelty incorporated thanks to the coupling with ngspice. To validate this scenario, we have used the setup shown in Fig. 6(c). A two conductor line was

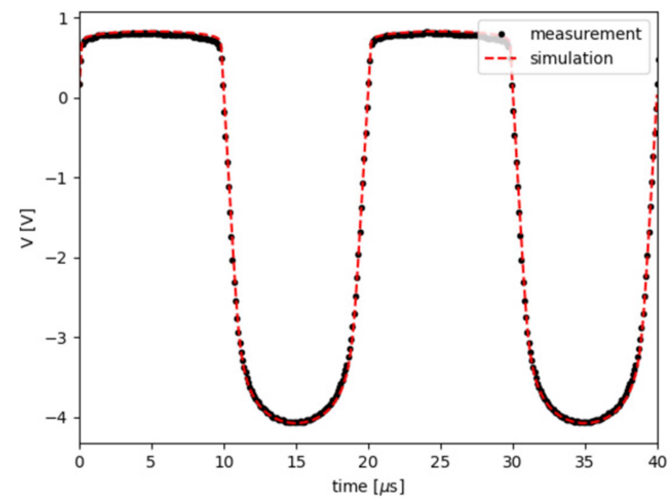

Fig. 7. Voltage drop at zener diode terminating the transmission line.

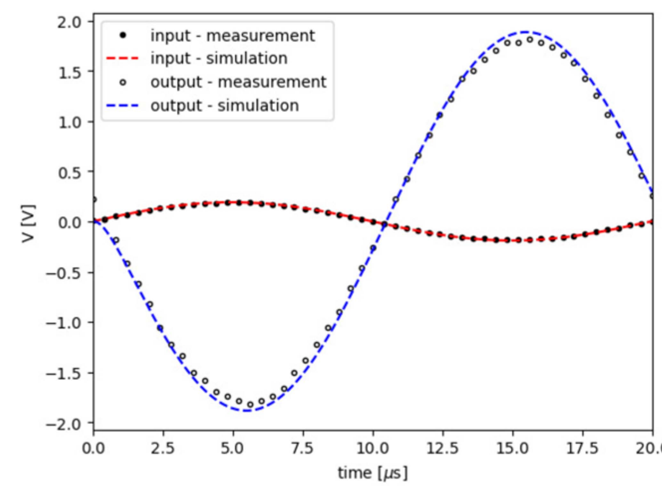

(a)

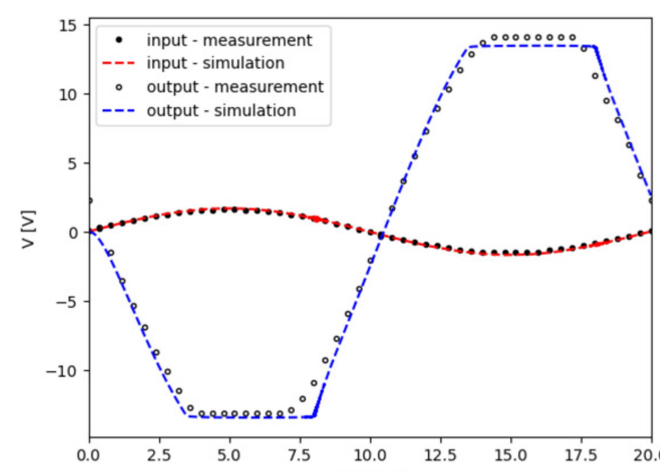

(b)

Fig. 8. Input and output voltage of a *Texas instruments* TL071cp operational amplifier [37] connected to the end of a transmission line. (a) Op-amp voltage out of saturation regime. (b) Op-amp voltage in saturation regime.

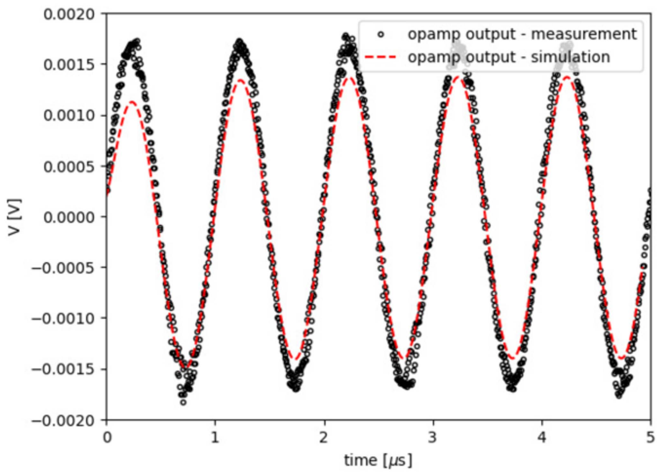

(a)

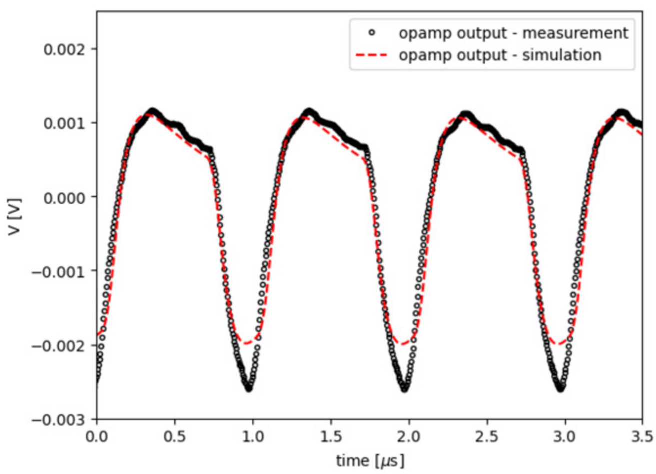

(b)

Fig. 9. Effect of cross-talk from a line excited by a sinusoidal or a pulse signal on a line terminated on a *Texas instruments* TL071cp operational amplifier [37]. (a) Op-amp output voltage with the line excited by a sinusoidal signal. (b) Op-amp output voltage with the line excited by a pulse wave.

excited with a source on the extreme of one of the wires, and the output voltage of an op-amp attached to the other wire is measured. The op-amp is mounted on a breadboard, where there are soldered tracks and some other components. Hence, a 1.75-n F capacitance has been added to represent the total parasitic capacitance between the breadboard with the op-amp and ground, which is not present in the component model.

Two different excitation signals were used: a sinusoidal signal and a pulse train, to have a case more representative of signals in digital systems. Since the induced voltages are proportional to the amplitude and the frequency of the source signal, we used a frequency of $f = 1\text{ M Hz}$ and an amplitude of $V_{pp} = 20\text{ V}$ in order to achieve a measurable cross-talk. With the signals used in the previous sections the op-amp output voltage would have been below the sensitivity of our instruments. In the case of the pulse train, the pulses had a rise time, fall time, duration and frequency of $\tau_r = 75\text{ n s}$, $\tau_f = 75\text{ n s}$, $\tau_d = 250\text{ n s}$, and $f = 1\text{ MHz}$, respectively. Fig. 9 shows the output voltages of op-amp, compared to measured data.

IV. Conclusion

We have presented an MTL solver that interfaces with the circuit solver ngspice to treat line terminations and interconnections. Using a circuit simulator to treat the connections in the network allows to simulate connections made with nonlinear components and electronic components, whereas conventional FDTD MTL solvers restrict to a series of lumped connections with RLC elements. Both the MTL solver and the interface are open source and part a 3-D FDTD full-wave electromagnetic simulator, allowing to study the interaction of transient fields with cable bundles. We have validated this approach by comparing the simulation results with measurements in three different scenarios: a single line terminated with a diode, a single line terminated with an operational amplifier, and two-conductor line, where the receptor line is terminated with an operational amplifier. In all cases, the simulation results match the measured data. The proposed method enables the simulation of networks of MTLs, where the terminations and interconnections of the lines are not just lumped RLC components, but are electronic circuits. The latter is a better representation of real connections in wiring networks. Even though the MTL-ngspice solver can be used as a standalone simulator, its power lies in being integrated in a 3-D full-wave solver, allowing to study the interaction of transient fields with realistic cable systems embedded in transport and communication infrastructures. The explanation and validation of the full-wave solver coupled with the MTL solver subject of this work will be part of a future publication.

Acknowledgment

The authors want to thank Jesper Lansink Rotgerink for his computation of the LC parameters of the wire panel. Views and opinions expressed are however those of the author(s) only and do not necessarily reflect those of the European Union or Clean Aviation Joint Undertaking. Neither the European Union nor the granting authority can be held responsible for them

References

[1] K. Yee, “Numerical solution of initial boundary value problems involving Maxwell’s equations in isotropic media,” *IEEE Trans. Antennas Propag.*, vol. 14, no. 3, pp. 302–307, May 1966.

[2] A. Taflove and S. C. Hagness, *Computational Electrodynamics: The Finite-Difference Time-Domain Method*. Norwood, MA, USA: Artech House, 2005.

[3] M. Feliziani and F. Maradei, “Full-wave analysis of shielded cable configurations by the FDTD method,” *IEEE Trans. Magn.*, vol. 38, no. 2, pp. 761–764, Mar. 2002.

[4] G. G. Gutierrez et al., “On the design of aircraft electrical structure networks,” *IEEE Trans. Electromagn. Compat.*, vol. 58, no. 2, pp. 401–408, Apr. 2016.

[5] J. Wang, X. Han, K. Yang, Y.-S. Xia, and W.-Y. Yin, “Hybrid FDTD method for studying electromagnetic coupling effects of transmission line networks,” *IEEE Trans. Electromagn. Compat.*, vol. 59, no. 5, pp. 1650–1653, Oct. 2017.

[6] M. Brignone, D. Mestriner, R. Procopio, A. Piantini, and F. Rachidi, “On the stability of FDTD-based numerical codes to evaluate lightning-induced overvoltages in overhead transmission lines,” *IEEE Trans. Electromagn. Compat.*, vol. 62, no. 1, pp. 108–115, Feb. 2020.

[7] A. Tatematsu and A. Yamanaka, “Three-dimensional FDTD-based simulation of lightning-induced surges in secondary circuits with shielded control cables over grounding grids in substations,” *IEEE Trans. Electromagn. Compat.*, vol. 65, no. 2, pp. 528–538, Apr. 2023.

[8] C. Paul, "Incorporation of terminal constraints in the FDTD analysis of transmission lines," *IEEE Trans. Electromagn. Compat.*, vol. 36, no. 2, pp. 85–91, May 1994.

[9] A. Orlandi and C. Paul, "Fdtd analysis of lossy, multiconductor transmission lines terminated in arbitrary loads," *IEEE Trans. Electromagn. Compat.*, vol. 38, no. 3, pp. 388–399, Aug. 1996.

[10] A. Orlandi and C. Paul, "An efficient characterization of interconnected multiconductor-transmission-line networks," *IEEE Trans. Microw. Theory Techn.*, vol. 48, no. 3, pp. 466–470, Mar. 2000.

[11] Z. Tong, L. Sun, L. M. D. Angulo, S. G. García, and J. Luo, "Multiresolution time-domain analysis of multiconductor transmission lines terminated in linear loads," *Math. Prob. Eng.*, vol. 2017, 2017, Art. no. 9845702. [Online]. Available: http://hdl.handle.net/10481/50230

[12] A. Demurov et al., "Fast simulation of large-scale cable systems by hybridization of MTL, MNA and FDTD methods," in *Proc. 2018 Int. Symp. Electromagn. Compat.*, 2018, pp. 844–848.

[13] L. Weiss and R. N. McDonough, "Prony's method, z-transforms, and pade approximation," *SIAM Rev.*, vol. 5, no. 2, pp. 145–149, 1963. [Online]. Available: http://www.jstor.org/stable/2027478

[14] F. Hildebrand, *Introduction to Numer. Anal.: Second Ed.*, in Series Dover Books on Mathematics. Garden City, NY, USA: Dover Pub., 2013. [Online]. Available: https://books.google.es/books?id=ic2jAQAAQBAJ

[15] M. Sarto, "A new model for the FDTD analysis of the shielding performances of thin composite structures," *IEEE Trans. Electromagn. Compat.*, vol. 41, no. 4, pp. 298–306, Nov. 1999.

[16] M. Celik, A. Cangellaris, and A. Yaghnour, "An all-purpose transmission-line model for interconnect simulation in spice," *IEEE Trans. Microw. Theory Techn.*, vol. 45, no. 10, pp. 1857–1867, Oct. 1997.

[17] Altair Engineering Inc, "Altair feko." Accessed: Apr. 19, 2025. [Online]. Available: www.altair.com/feko

[18] Electro Magnetic EMA Inc Applications, "MHARNESS, a cable harness EM solver," Denver, CO, USA. Accessed: Apr. 19, 2025. [Online]. Available: https://www.ema3d.com/mharness-is-a-cable-harness-em-solver/

[19] M. Paolone, C. A. Nucci, and F. Rachidi, "A new finite difference time domain scheme for the evaluation of lightning induced overvoltages on multiconductor overhead lines," in *Proc. Int. Conf. Power Syst. Transients*, 2001, pp. 596–602.

[20] Ngspice, "Ngspice - mixed model - mixed level circuit simulator." Accessed: Apr. 19, 2025. [Online]. Available: https://ngspice.sourceforge.io/authors.html

[21] H. Vogt, G. Atkinson, and P. Nenzi, *Ngspice User's Manual, Version 44plus (Ngspice Develop. Version)*, Apr. 2025. Accessed: Apr. 19, 2025. [Online]. Available: http://ngspice.sourceforge.net/docs.html

[22] "OpenSEMBA, open-source repository of codes for solving electromagnetic problems (FDTD)." Accessed: Apr. 19, 2025. [Online]. Available: https://github.com/OpenSEMBA/fdtd

[23] C. R. Paul, *Analysis of Multiconductor Transmission Lines*, Hoboken, NJ, USA: Wiley, 2007, ch. 2, Section 2.4.

[24] C. R. Paul, *Analysis of Multiconductor Transmission Lines*. Hoboken, NJ, USA: Wiley, 2007.

[25] Z. Mazloom, N. Theethayi, and R. Thottappillil, "Method to include lumped devices in multi-conductor transmission line system models," in *Proc. 2009 IEEE Power Energy Soc. Gen. Meeting*, 2009, pp. 1–6.

[26] "GCEM - Grup de Compatibilitat Electromagnètica de la Universitat Politècnica de Catalunya." Accessed: Apr. 19, 2025. [Online]. Available: https://ieb.eel.upc.edu/en/research-areas/electromagnetic-compatibility-emc

[27] "GEG - Grupo de Electromagnetismo de Granada." Accessed: Apr. 19, 2025. [Online]. Available: https://geg.ugr.es/

[28] M. R. Cabello et al., "SIVA UAV: A case study for the EMC analysis of composite air vehicles," *IEEE Trans. Electromagn. Compat.*, vol. 59, no. 4, pp. 1103–1113, Aug. 2017.

[29] L. D. Angulo, M. R. Cabello, J. Alvarez, A. R. Bretones, and S. G. Garcia, "From microscopic to macroscopic description of composite thin panels: A roadmap for their simulation in time domain," *IEEE Trans. Microw. Theory Techn.*, vol. 66, no. 2, pp. 660–668, Feb. 2018.

[30] A. G. Bravo et al., "Time domain simulation of common mode ferrite chokes at system level," *IEEE Trans. Electromagn. Compat.*, vol. 65, no. 6, pp. 1900–1908, Dec. 2023.

[31] C. R. Paul, "n wires above an infinite, perfectly conducting plane," in *Analysis of Multiconductor Transmission Lines*, Hoboken, NJ, USA: Wiley, 2007, ch. 5, section 5.2.1.2.

[32] R. Schwarz, "R&S RTC1000 oscilloscope," Oct. 2024. Accessed: Apr. 19, 2025. [Online]. Available: https://www.rohde-schwarz.com/es/productos/test-y-medida/osciloscopios/rs-rtc1000-oscilloscope_63493-515585.html

[33] Keysight, "33220a function/arbitrary waveform generator, 20 MHz," May 2015. Accessed: Apr. 19, 2025. [Online]. Available: https://www.keysight.com/us/en/product/33220A/function-arbitrary-waveform-generator-20-mhz.html

[34] R. Holland and L. Simpson, "Finite-difference analysis of EMP coupling to thin struts and wires," *IEEE Trans. Electromagn. Compat.*, vol. EMC-23, no. 2, pp. 88–97, May 1981.

[35] Cordell Audio,"SPICE Models." Accessed: Apr. 19, 2025. [Online]. Available: https://www.cordellaudio.com/book/spice_models.shtml

[36] Ngspice, "Models for ngspice - micro-cap 12." Accessed: Apr. 19, 2025. [Online]. Available: https://ngspice.sourceforge.io/model-parameters/MicroCap-LIBRARY.7z

[37] Texas Instruments, "Tl07xx low-noise fet-input operational amplifiers," Tech. Rep. SLOS080V, Apr. 2023. Accessed: Apr. 19, 2025. [Online]. Available: https://www.ti.com/lit/ds/symlink/tl071.pdf?ts=1725284536138

[38] Texas Instruments, "Tl071, tl071a, tl071b pspice model." Accessed: Apr. 19, 2025. [Online]. Available: https://www.ti.com/lit/zip/sloj066

Alberto Gascón Bravo received the M.Sc. and Ph.D. degrees in physics from the University of Granada, Granada, Spain, in 2009 and 2014, respectively.

He is currently a Postdoctoral Researcher with the Department of Electromagnetism and Matter Physics, the University of Granada. He has worked in the fields of astroparticle physics and accelerator physics. His current research interests include electromagnetic compatibility, computational electromagnetism, and machine learning.

Luis Manuel Diaz Angulo (Member, IEEE) received the M.Sc. and Ph.D. degrees in physics, and the M.Sc. degree in electronics engineering from the University of Granada, Granada, Spain, in 2008, 2014, and 2015, respectively.

He is currently an Associate Professor with the Department of Electromagnetism and State Matter, University of Granada. He has worked in time domain computational electromagnetics, especially discontinuous Galerkin and finite-differences. The main applications of these methods have been in the areas of electromagnetic compatibility, and material characterization

Ferran Silva (Senior Member, IEEE) received the M.Sc. and Ph.D. degrees from the Universitat Politècnica de Catalunya (UPC), Barcelona, Spain, in 1989 and 1997, respectively.

He is currently an Associate Professor with the Department of Electronic Engineering, UPC. From 1993 to 2024, he served as Head of the Electromagnetic Compatibility Group (GCEM-UPC)with the UPC. He has authored or coauthored over 180 publications on EMC in journals, conferences, and books, and has participated in 37 research projects related to EMC. His research interests include electromagnetic compatibility (EMC) in the near-field and time domain, with applications in transport, medical, and industrial sectors. Dr. Silva has twice served as Chair of the IEEE EMC Society Spanish Chapter. Furthermore, he is a Member of the EMC Spanish Standardization Committees SCTC77-210 and CTN208 SCCISPR210 A. He chaired the 2006 and 2019 editions of the EMC Europe International Symposium in Barcelona. Since 2004, he has been a Member of the EMC Europe International Steering Committee.

Marcos Quílez (Member, IEEE) received the Ingeniero de Telecomunicación degree and Doctor Ingeniero de Telecomunicación degree from the Universitat Politècnica de Catalunya (UPC), Barcelona, Spain, in 1997 and 2004, respectively.

He is an Associate Professor with the Department of Electronic Engineering, UPC, where he teaches courses on electronic systems, sensors and signal conditioning, and electromagnetic compatibility (EMC). His research interests include the area of Electromagnetic Compatibility and Electronic Instrumentation.

From 1996 to 2005, he was with the Electromagnetic Compatibility Group (GCEM_UPC), until he joined the Instrumentation, Sensors and Interfaces research Group (ISI). Since 2016, he shares his research activity with both groups. His research interests include design for EMC, near field measurements and sensor applications for the agri-food industry.

Kenan Tekbaş (Member, IEEE) received the M.Sc. degree in communication engineering and the Ph.D. degree in electrical and electronic engineering from The University of Manchester, Manchester, U.K., in 2012 and 2017, respectively.

From 2022 to 2024, he worked as a Marie Skłodowska-Curie Postdoctoral Fellow with the Department of Electromagnetism, University of Granada, Granada, Spain. His research interests include computational electromagnetics, the finite-difference time-domain method, numerical modeling of magnetic materials, and bioelectromagnetism.

Salvador G. García (Senior Member, IEEE) received the M.Sc. and Ph.D. degrees (with extraordinary award) in physics from the University of Granada, Granada, Spain, in 1989 and 1994, respectively.

He is a Full Professor with the Department of Electromagnetism and Matter Physics, University of Granada. In 2010, he co-founded the startup Elemwave devoted to numerical solver development and EM consultancy. He has published over 90 refereed journal articles and book chapters and led several national and international projects. His current research interests include computational electromagnetics, electromagnetic compatibility, RCS, antenna design, and material analysis.